7-1-2016

DEVELOPMENT OF OLIGO(p-PHENYLENE EHYNYLENE)(OPE) APPLICATIONS AGAINST CHEMICAL AND BIOLOGICAL THREATS

Suhyun Yoon

[redacted]

[redacted]

This thesis is approved, and it is acceptable in quality and form for publication:

Approved by the Dissertation Committee:

[redacted]

[redacted]

[redacted]

DEVELOPMENT OF OLIGO(*p*-PHENYLENE EHYNYLENE)(OPE)

APPLICATIONS AGAINST CHEMICAL AND BIOLOGICAL THREATS

by

SUHYUN YOON

B.S. Chemistry, Sejong University, Seoul, South Korea, 2013

THESIS

Submitted in Partial Fulfillment of the
Requirements for the Degree of

Master of Science
Chemistry

The University of New Mexico
Albuquerque, New Mexico

July, 2016

DEVELOPMENT OF OLIGO(*p*-PHENYLENE EHYNYLENE)(OPE) APPLICATIONS AGAINST CHEMICAL AND BIOLOGICAL THREATS

by

Suhyun Yoon

M.S. Chemistry, The University of New Mexico, 2016

ABSTRACT

Four new applications of oligo-phenylene ethynylene (OPE) and poly-PE (PPE) compounds for detection and destruction of biological and chemical threats have been investigated. Mixed surfaces composed of PPEs and a thermoswitchable polymer were created, and were shown to be able to capture, kill, and reversibly release pathogenic bacteria. In order to develop fluorescent sensors for CW agents, the spectral changes of OPEs with surfactants and malathion (a simulant for nerve agents) were measured. Formation of OPE-dimers in the presence of surfactants can cause fluorescence enhancement (turn-on) or quenching (turn-off). Among six positive and negative OPEs, only OPEs with ethyl ester (COOEt) functional groups show fluorescence enhancement in the presence of surfactants, and quenching in the presence of malathion. In order to improve the lower detection limit (which is about nM) and specificity, a new OPE molecule with oximate ($R\text{-}N{=}O^-$) functional groups is being synthesized and tested. Finally, PE compounds were investigated as potential dyes for two-photon microscopy, and were found to be cell-penetrant, to have a good two-photon excitation cross-section, and hence to be useful as a nucleic acid stain for mammalian cells.

TABLE OF CONTENTS

LIST OF FIGURES……vi

CHAPTER 1 – INTRODUCTION…..……1

1.1 Motivation and Outline of research projects…..……1

1.2 Background……..…....2

CHAPTER 2 – SWITCHABLE BIOCIDAL SURFACES……....…4

2.1 Introduction…….....4

2.2. Results……..5

2.2.1. Fabrication and Nanoscale Morphology…….....5

2.2.2. Killing and Release Function…….....9

CHAPTER 3 – SENSORS FOR CHEMICAL WARFARE AGENTS……11

3.1. Introduction…….11

3.2. Background…….11

3.2.1. ACh, AChE, and the Aging Process caused by OP compounds…….11

3.2.2. OPE-Surfactant Complexes as Sensors……..13

3.3. Materials and Methods……15

3.4. Results……..…18

3.4.1. Ex and Em Spectra of Positve OPEs vs SDS…….….18

3.4.2. Ex and Em Spectra of Postive OPE and SDS vs Malathion……....20

3.4.3. Ex and Em Spectra of Negative OPE vs TTAB……...22

3.4.4. Ex and Em Spectra of Negative OPE and TTAB vs Malathion……..22

CHAPTER 4 – STUDIES ON OXIMATES AND FLOURESCENCE CHANGES…..26

4.1. Background…….26

4.2. Oxime-OPEs as Selective Sensors ……..……28

4.2.1. Synthetic Procedure……..…..29

CHAPTER 5 – DETECTING CHEMICAL WARFARE AGENTS IN CELLS…….....30

5.1. Background…….30

5.2. Materials and Methods……33

5.3. Results…….34

CHAPTER 6 – CONCLUSIONS…….……...39

REFERENCES……...……..41

LIST OF FIGURES

Figure 1. AFM Tapping Mode Height Images of Active Films on Borosilicate Glass Substrates……..….7

Figure 2. Structure of the Random Mixed CPE and PNIPAAm Surfaces……....8

Figure 3. Fluorescence Images of Bacteria and Combined CPE/PNIPAAM Surfaces…….....9

Figure 4. ACh, AChE and the Inhibition Caused by Organophosphorus Compounds…..…..12

Figure 5. UV-visible Absorbance Spectra with 20uM PE-SO_3-H with Surfactants……....14

Figure 6. Absorbance and Emission Spectra with 1.4uM S-OPE-2-COOEt with DLPG…...15

Figure 7. Positively Charged PE-backboned Oligomers and Polymer……...…16

Figure 8. Negatively Charged PE-backboned Oligomers……16

Figure 9. Molecular Structures of Surfactants and Malathion……....17

Figure 10. A Table of OPE Excitation Wavelengths for Emission Spectra……..…18

Figure 11. Emission and Excitation Spectra of 2uM Positive OPEs with SDS……...19

Figure 12. Emission and Excitation Spectra of 2uM Positve OPEs and 1.98uM SDS with malathion……21

Figure 13. Emission and Excitation Spectra of 2uM Negative OPEs with TTAB…….24

Figure 14. Emission and Excitation Spectra of 2uM Negative OPEs and 1.96uM TTAB with malathion……25

Figure 15. Absorption and Emission Spectra of Coumarin-Oximate Compounds with various amount of diioprypylfluorophosphate(DFP)……..……26

Figure 16. Reaction Mechanisms of 4-PAM with Chemical Warfare Agents……..…..27

Figure 17. A Scheme of Different Fluorophore with Various Reactive Functional Groups...27

Figure 18. Observation of Fluorescent Color Changes of Different Compounds shown on figure 17…….28

Figure 19. Synthesis Steps of an End-Only Oximated OPE Molecules……....29

Figure 20. A Diagram of One-Photon and Two-Photon Excitations……..31

Figure 21. Illustration of Focuses with One-Photon and Two-Photon Excitations……..….32

Figure 22. Images of on-OPE Treated 3t3 Cells with Syto 21 Stain……..35

Figure 23. Images of 3t3 Cells with 10ug/ml OPE Treatment for 30 Minutes……..…36

Figure 24. Images of 3t3 cells Treated with Various OPE Concentrations……37

CHAPTER 1. INTRODUCTION

1. 1. Motivation and Outline for Research Projects

Worldwide, threats from chemical and biological warfare (CBW) agents have increased in recent years.[1] Biological agents such as bacteria pose risks that range from relatively limited infections against soldiers (e.g. *Bacillus anthracis*, anthrax) to potentially unlimited epidemics in the general population (e.g., *Yersinia pestis*, bubonic plague). Chemical agents pose risks that range from skin irritation and blistering (e.g., chlorine, mustard agents) to rapid and painful death (e.g. organophosphorus (OP) nerve agents such as sarin, soman, VX). In order to defeat potential CBW attacks, the importance of developing methods to detect and protect against such agents has also risen.

The project outlined below includes four efforts to develop such methods, all based on a class of fluorescent, biocidal molecules called oligo *p*-phenylene ethynylenes (OPEs) and poly *p*-phenylene ethynylenes (PPEs). In the first effort a new multifunctional surface was developed that can initially bind bacterial cells, then kill them (using the light-activated biocidal properties of PPEs), and then, by raising temperature slightly, release them to make the surface ready for another round of decontamination. In the second effort, OPEs were used to create a fluorescence-based sensor for malathion (a common pesticide and simulant for for organophosphorous nerve agents). In this case an OPE molecule senses malathion by forming a complex in the presence of a surfactant molecule. The third effort is still preliminary. It aims to improve the sensitivity and specificity of the CW sensor by synthesizing a new OPE molecule that is capable of reacting with CW agents to form a covalent complex. Finally, the

fourth effort explored the possibility of using OPEs and PPEs as sensors and detectors for CW agents inside cells and tissues, using two-photon fluorescence microscopy.

1. 2. Background

Poly phenylene ethynylenes, whose synthesis was made accessible by the discovery by Sonogashira and co-workers in 1975 of a facile bond-forming reaction between terminal acetylene and aryl or vinyl halide in the presence of catalytic Pd(0) and Cu(I),[2] have been extensively explored for a variety of useful properties. Besides applications in organic photovoltaics,[3] their photosensitizer properties have been explored to make light-activated antimcirobials,[4] and their remarkable quenching and self-assembly have been used to develop sensors[5].

The OPEs and PPEs have been shown to have the ability to kill bacteria by (at least) two mechanisms: a) disrupting cell membranes, and b) generating reactive oxygen species using visible light.[6] The first mechanism works under all conditions. The second (usually more efficient) mechanism works whenever OPEs or PPEs are exposed to visible light. Figures 8 and 9 show the structures of some representative OPEs and PPEs. The side chains (often quaternary amines) provide both solubility and the ability to kill in the absence of light. The conjugated backbone acts as the chromophore necessary for either fluorescence or the photo-generation of reactive oxygen species by which OPEs and PPEs become light-activated biocides. Thus OPEs and PPEs have a light-activated biocidal property that can be used to make otherwise passive surfaces into active "devices" that can sterilize biological warfare agents and (potentially) destroy chemical warfare agents. The investigation of these surfaces forms the first part of this work.

The utility of poly- and oligo-PEs has been demonstrated in a variety of sensing systems[7], including DNA detection[8], enzyme activity assays[9, 10], and as stains for amyloid.[11] Using the known properties of variously substituted OPEs to form H- and J- aggregates with submicellar concentrations of surfactants, the second part of this work attempts to demonstrate detection of organophosphorus nerve agent by non-covalent disruption of the aggregate. The third part extends the sensitivity and selectivity of this assay by designing OPEs with a component that binds covalently to the phosphoester.

PE's have also been investigated as cell-penetrant dyes for two-photon microscopy, using their large size and tendency to self-aggregate as a method to increase cross-section of the two-photon absorption nonlinear optical process.[12] The fourth part of the work discusses the promising advantages of two-photon microscopy and reports the effective intracellular detection of various OPEs with this technique.

CHAPTER 2. SWITCHABLE BIOCIDAL SURFACES

2.1 Introduction

In the first effort a new type of surface was developed. By combining both the light-activated biocidal polymer PPE-DABCO with thermally-switchable Poly(N-isopropylacrylamide) (PNIPAAm), the surface can first capture bacteria, then kill them, then release them at lower temperature. The surface consists of two active materials: poly(p-phenylene ethynylene)-based polymers, which can inactivate a broad range of microbes and pathogens, and poly(N-isopropylacrylamide), which can convert between an hydrophobic "capture" state and a hydrophilic "release" state, in a patchwork arrangement. The combination of these materials creates a surface that can both trap microbes in a switchable way and kill surface-bound microbes efficiently.

OPEs and CPEs are highly disruptive against microbial cell walls, and they have been demonstrated to kill Gram-negative bacteria, Gram-positive bacteria (including biofilms, spores, viruses and fungi). OPEs and PPEs are also light-activated; exposure to light sensitizes the production of singlet oxygen that reacts to form various species that oxidize available biological redox sites, disrupting the physical structure and metabolism of the target organism. This light- and dark-environment killing activity is highly effective in solution, but for real-world applications a surface-based approach would be more practical.[13]

Control of cellular adhesion to surfaces through control of surface free energy is a useful approach to inhibiting biofilms. PNIPAAm undergoes an entropically driven phase transition from a hydrophobic, collapsed state above about 32 °C to a hydrophilic expanded state at low temperature. This change has been shown to modify the adhesion of cells to a PNIPAAm surface to a significant extent.[14]

This section describes the fabrication, characterization, and testing of an active, nanostructured surface functionalized with both biocidal CPEs and temperature-switchable PNIPAAm. The surface was prepared by a combined approach of sequential layer-by-layer polyelectrolyte deposition and surface-initiated atom transfer radical polymerization. The resulting surface exhibits both characteristics of the biocidal CPEs and temperature-switchable PNIPAAm. The surface topology and patterning of different polymers was characterized with atomic force microscopy. Bacterial cells, which were deposited onto the surfaces, were evaluated for killing by live/dead staining with a cell-permeant and cell-impermeant nucleic acid stain, allowing for determination of the membrane-compromised individuals by confocal microscopy. Cell release rates were determined by fluorescence microscopy after washing with 5 mL of cold water.

2.2. Results

2.2.1. Fabrication and nanoscale morphology

Films of CPEs can be formed controllably using a layer-by-layer (LbL) strategy, in which an initial layer of a CPE polycation (PPE-DABCO) is first physisorbed to a glass substrate, then a second layer of a CPE polyanion (PPE-SO3) is physisorbed on top, followed by a third layer of a CPE polycation (Figure 2). A higher degree of surface roughness is achieved by introducing a multilayer film, rather than just a single layer of cationic polymer, which is optimal for the binding of bacteria.

Figure 1a shows such an LbL CPE film imaged by AFM (1.5 bilayers, substrate/PPE-DABCO/PPESO3/PPE-DABCO, on a glass coverslip) on a wide scale (main image, 5 μm × 5 μm) and on a 10× magnified scale (inset, 500 nm × 500 nm). On the wide scale the film

appears quite smooth, with only subnanometer roughness. By scratching the film with the AFM tip, it was possible to show that the overall film is about 5 nm thick. A higher resolution AFM image of the CPE film is shown in the inset of Figure 1a. Here, it can be seen that the surface is populated by distinct nodular structures averaging about 10−20 nm in size. The nodules are presumably due to aggregated CPE chains, either with themselves or with the polymer of opposite charge. It is also apparent that the top layer of PPE-DABCO may not be completely continuous; some regions of the surface descend by about 1.5 nm from the average height of the top layer, which is enough to reach down to the PPE-SO3 layer below. Statistically, such regions of deficiency may extend to the glass substrate. Overall, the structure of the CPE LbL film as seen by AFM is consistent with the model shown in Figure 2, where regions with 1.5 bilayers are mixed with regions with fewer layers, including some regions of bare glass.

Surface-polymerized PNIPAAm films have often been fabricated in the three-step process. First, a free radical polymerization initiator is first attached to a glass substrate using a silane linkage; then PNIPAAm is grown from these initiator sites using atom transfer radical polymerization in alcoholic solution. Figure 2b shows an AFM image of a PNIPAAm film grown in this way. The main image shows the film on a wide scale, and the inset shows a higher resolution image. On both scales the film appears smooth and continuous, with a grain structure of about 10 nm visible at high resolution. It was not possible to measure the PNIPAAm film thickness directly in this case. The film could not be scratched, consistent with covalent grafting of the polymer chains to the glass. Films made under similar conditions were reported to have thickness of less than 10 nm. From images like those in Figure 1a it was expected that thin LbL films of CPEs (especially films with only 1.5 bilayers) on glass might

be discontinuous, having small regions of uncoated, solvent-exposed glass substrate surrounded by CPE. If so, a combined CPE/PNIPAAm film could be created by first depositing a thin LbL film, then attaching ATRP initiators in these exposed regions. Control experiments in which CPE LbL films were exposed to the polymerization conditions (toluene solvent overnight and alcohol solvent) showed no damage to the CPE LbL films. Figure 1c shows a mixed CPE/PNIPAAm film fabricated by first doing a 1.5 BL deposition, followed by surface grafting of PNIPAAm. Both the wide scale main image and the high-resolution inset show a pattern of relatively large raised features on a smoother background. The size of these raised features varies widely, from about 5 nm to more than 50 nm in lateral dimension, and from less than 1 nm to about 5 nm in height. Overall this structure is consistent with the model shown in Figure 2, where plumes of PNIPAAm have grown from a set of discrete sites where ATRP initiators where located originally. In Figure 2 c the fractional surface coverage by PNIPAAm appears to be about 50%. In other samples with longer growth times, much higher surface coverage were seen, including some large areas (~1 μm) of nearly continuous PNIPAAm overgrowth of the CPE film. Overall, AFM shows that the 1.5 BL CPE film remains intact following exposure to acetone and methanol.

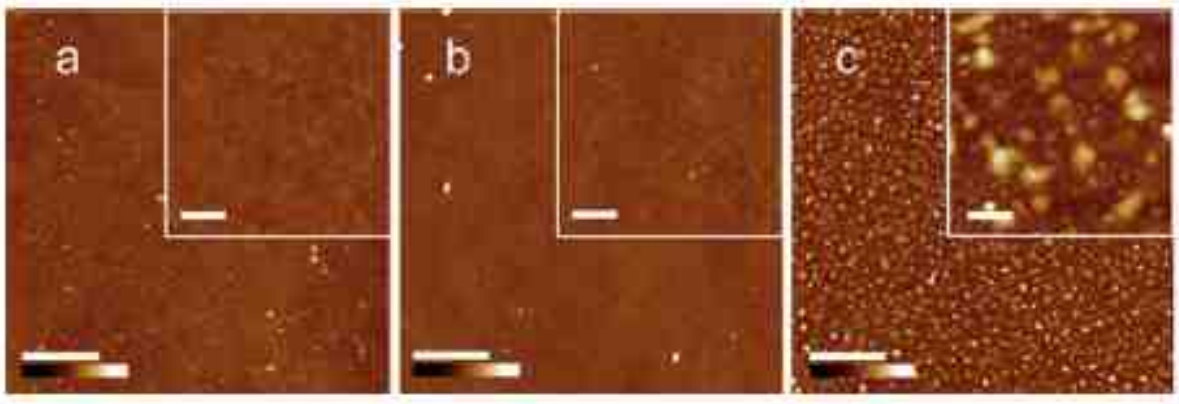

Figure 1. AFM tapping mode height images of active films on borosilicate glass substrates: (a) LbL CPE film with the structure: substrate//PPE-DABCO//PPE-SO_3//PPE-DABCO.

The main image is 5 μm × 5 μm (scale bar 1 μm). The inset image is 500 nm × 500 nm (scale bar 100 nm). Height scale color bar is 25 nm from black to white. (b) Surface-polymerized film of PNIPAAm alone. Scale and color bars as in (a). (c) Mixed CPE/PNIPAAm film created by forming the LbL layers in (a), followed by surface polymerization of PNIPAAm as in (b). Scale and color bars as in (a). Adapted from Pappas et al.

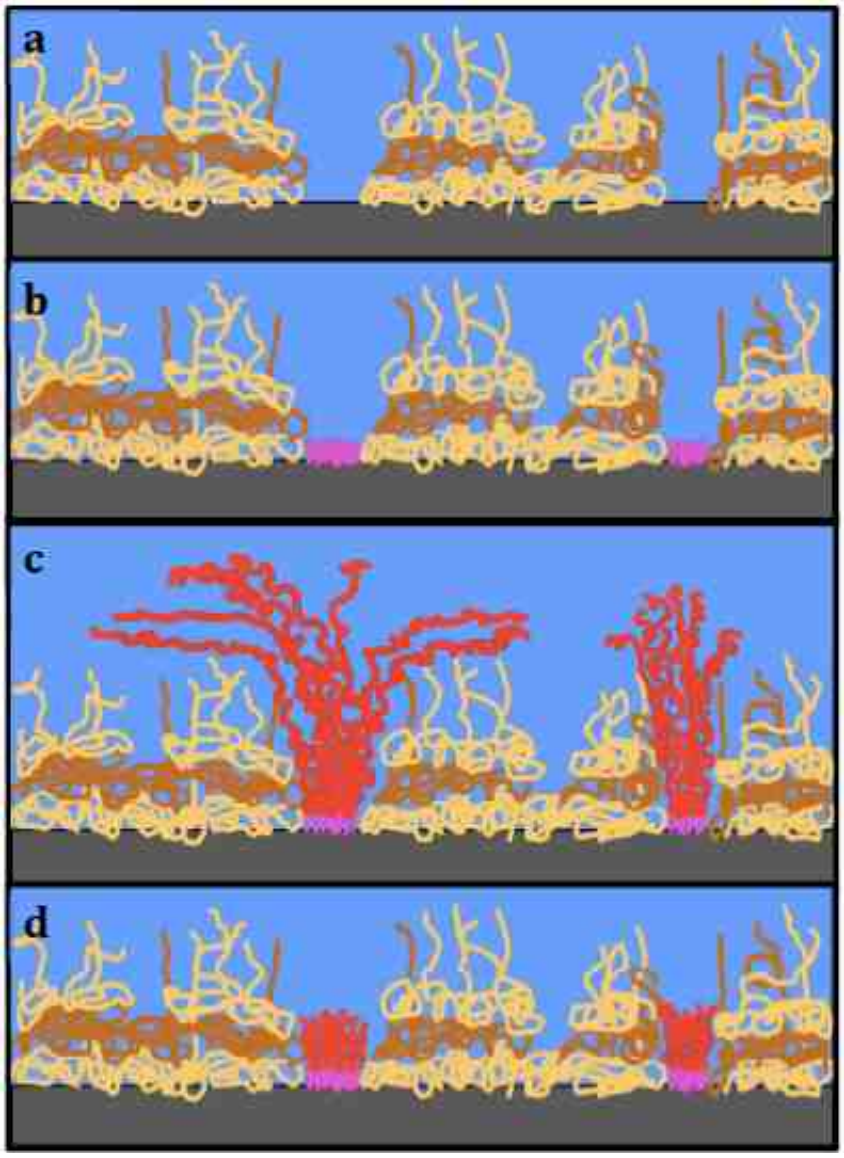

Figure 2. Structure of the random mixed CPE and PNIPAAm surfaces. (a) Layer-by-layer film formed from PPE-DABCO (light brown) and PPE-SO_3 (orange) on a glass surface (gray). (b) 3 layer CPE surface with silane linkers (pink) attached to the glass substrate via gaps in the CPE coverage. PNIPAAm (red) polymerized from the silane linkers at 4 °C (c) and 37 °C (d). The PNIPAAm extends beyond the CPE layers to create the plumes and surface coverage observed in the AFM images. Adapted from Pappas et al.

2.2.2. Killing and Release Function

The ability of mixed CPE/PNIPAAm surfaces to inactivate bacterial cells and then release them was tested by a) depositing cells on the surface at high temperature (37 °C), b) exposing the adsorbed bacteria to visible light for a fixed length of time, c) staining the cells with “live” and “dead” fluorescent stains and imaging by confocal fluorescence microscopy, and finally d) releasing the cells with a cold-buffer rinse (4 °C). Live-dead stained confocal microscopy indicated a peak killing level of around 80% for the light-activated PNIPAAm/PPE surfaces against both bacterial species. After rinsing with 5 mL of cold buffer, around 90% of the cells were removed from the PNIPAAm/CPE mixed surface, as shown in Figure 3. No cells were removed with similar rinsing from untreated glass or pure CPE-coated surfaces.

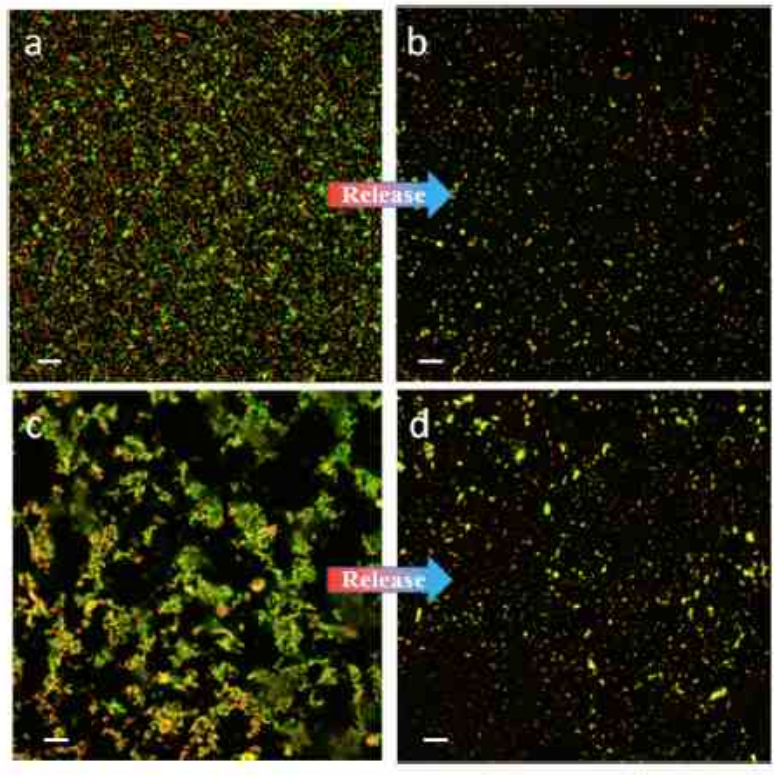

Figure 3. Fluorescence images of bacteria on combined CPE/ PNIPAAm surfaces. Bacteria were adsorbed from suspension at a concentration of 1×10^7 cells/mL. (a) E. coli after adsorption for 1 h at 37 °C and 1 h exposure to 420 nm light. Green cells are living; yellow or red cells are dead. (b) E. coli substrate, shown in (a), following rinsing with 5 mL of 4 °C water. (c) S. aureus after adsorption for 1 h at 37 °C and 1 h exposure to 420 nm light. (d) S.aureus substrate shown in (c) following rinsing with 5 mL of 4 °C water. Scale bars denote 20 μm in all images. Adapted from Pappas et al.

CHAPTER 3. SENSORS FOR CHEMICAL WARFARE AGENTS

3.1. Introduction

Against chemical warfare agents threat, in addition to the applications of OPEs against biological warfare, an approach has been arising: detecting CW agents by observing fluorescence color changes with low detection limit by disruption of a dye/surfactant pre-micellar complex. In order to develop sensors, the fluorescent changes of OPEs needs to be tested. First, some background on CW agents, their chemistry, and the mechanisms used to detect them should be presented.

3.2. Background

3.2.1. ACh, AChE, and the aging prosess caused by organophosphorus compounds

Many of the most dangerous CW agents are covalent inhibitors of acetylcholinesterase (AChE) which function by very similar chemistry, and hence have similar chemical properties overall. Acetylcholine (ACh) and AChE play key roles in the nervous system, especially at the synapse between nerves and muscles. Acetylcholine is a neurotransmitter that, among other roles in the central and peripheral nervous system, delivers the signal for muscle contraction from the neuronal to the muscular side of the neuromuscular synapse. After acetylcholine molecules are released from the neuron into the synaptic cleft, they bind to receptors on the opposite side of the synapse. This opens the Na+/K+ channels of nicotinic acetylcholine receptors, which depolarizes the membrane and initiates a cascade leading to muscle contraction (Figure 4a).[15] AChE is a hydrolase that breaks ACh into acetate and

choline. AChE plays a crucial role in vertebrate motion by degrading free ACh in the neuromuscular junction, allowing the muscles to eventually relax.

Organophosphorous compounds such as Sarin (GB), Soman (GD) and nerve agents (VX) are extremely dangerous because they irreversibly inhibit AChE. Even though AChE has high affinity for acetylcholine and reaction time is fast (necessary for adaptive function of the muscle response), the organophosphorus agents create strong covalent bonds with the active serine in the catalytic site of acetylcholinesterase, disabling the enzyme. Inhibition of AChE thus causes the ion channels on the muscle tissues to be excited. Eventually, the muscles go into permanent tension (Figure 4 (c)). Turnover and axonal transport of new AChE is not fast enough to recover normal synaptic function before death by asphyxia.

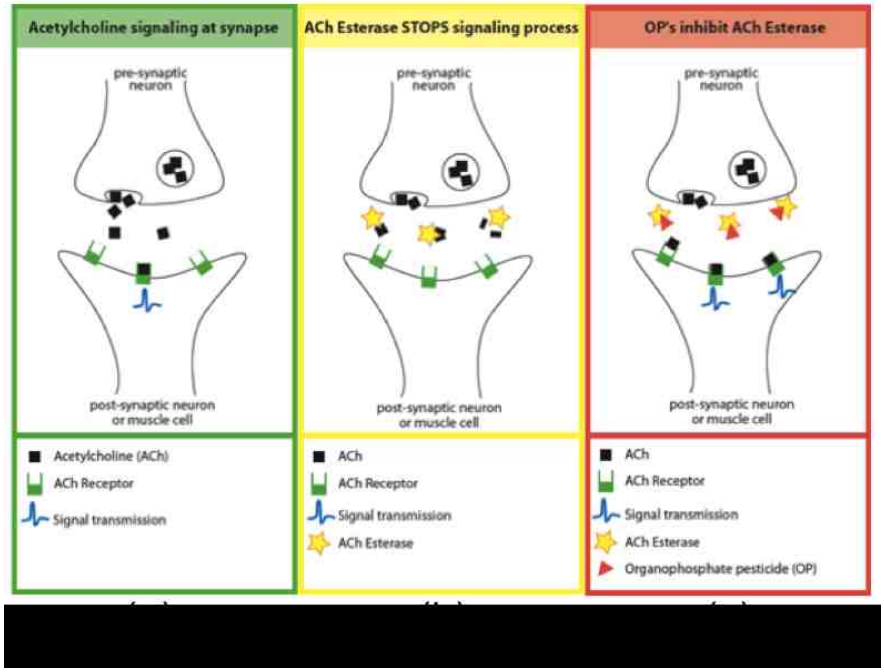

Figure 4. ACh, AChE and the aging caused by organophosphorous compounds. Adapted from Pediatric Environmental Health Specialty Unit(PEHSU) from University of Washington.

Fast detection of organophosphorus compounds in the air at low concentrations is extremely valuable, because swift administration of a reversible AChE inhibitor such as atropine, or a drug such as pralidoxime that reverses the covalent attachment, can prevent death and raise the LD50 of sarin by 7-14 fold.[16] Since deadly weapons such as sarin share their mechanism of function with relatively harmless pesticides such as malathion, differing mainly in their pharmacokinetics, it would be especially useful to be able to distinguish between organophosphorus compounds bearing different substituents.

3.2.2. OPE-surfactant complexes as sensors

A recently developed class of fluorescent molecules with phenylene - ethynylene (PE) backbones can act as excellent sensors for a class of CW simulant molecules (malathion and its derivatives) when in complex with an anionic surfactant at very low concentrations. Oligo phenylene ethynylenes (OPEs) have recently been shown to be both efficient fluorophores and (depending on details of structure) sources of photo-generated reactive oxygen species, especially singlet oxygen. As such, the OPEs are attractive candidates as both potential CW sensors and potential CW-destroying agents. Several OPE variants are able to detect the CW simulant malathion when in aqueous complex with small concentrations of surfactants such as sodium dodecyl sulfate (SDS). At the correct molar ratios, the combination of the OPE molecule with SDS and malathion appears to form a cooperative triple complex that varies sharply in its fluorescence properties over a narrow range of malathion concentrations. With some OPE/surfactant combinations the complex acts as a "turn off" detector—fluorescence intensity decreases with malathion concentration—while other combinations can act as "turn on" detectors—fluorescence intensity increases with malathion concentration.

Aggregation between molecules is caused by molecular interaction such as London dispersion, hydrophobic forces, and pi-pi and pi-cation interactions. Absorption or emission spectra of aggregates can be either blue shifted or red shifted with respect to the monomers. Dimers with the blue-shifted spectra are called H-aggregates, and dimers with red-shifted spectra are called J-aggregates. H and J-aggregates can be caused by parallel (plane to plane stacking) or alternating (head-to-tail) stacking.

Sensors for chemical warfare agents and mimics have been developed based on such property changes in dye molecules. Hill at al reported the fluorescence changes of charged oligo phenylene ethynylene compounds with surfactants and lipids.[9, 10] Adding TTAB in 20uM PE-SO_3-H in water solvent causes absorbance signal changes. Even though OPE absorbance spectra decreased (between 0uM and 60uM of TTAB concentrations) and then increased (up to 0.2mM), a strong red-shift occurs throughout, indicating steady J-aggregate formation (Figure 5). In addition, the fluorescent changes of S-OPE-2-COOEt molecules with various amounts of 1,2-dilauroyl-sn-glycero-3-phospho-(1′-rac-glycerol) (DLPG) also shows red-shifts caused by J-aggregate formation (Figure 6).

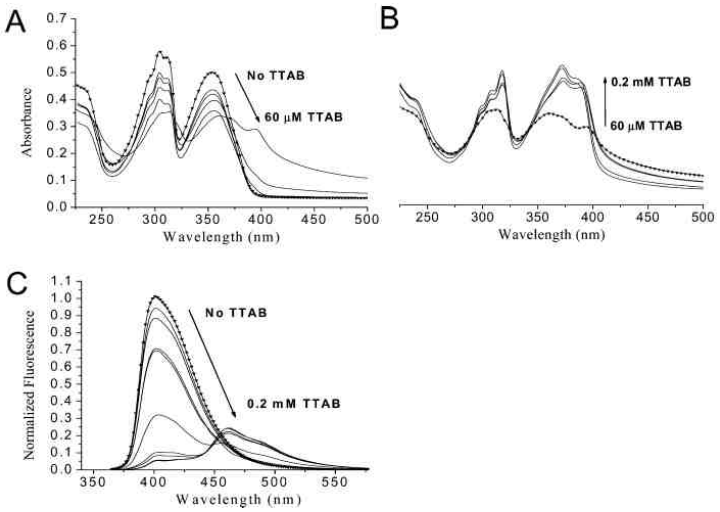

Figure 5. UV-visible absorbance spectra with 20uM PE-SO3-H (A) with various amount of TTAB (from 0 to 60uM) (B) with various amount of TTAB (from 60uM to 0.2mM) and

Emission spectra with 20uM PE-SO3-H with TTAB (from 0 to 0.2mM). Adapted from Hill et al.

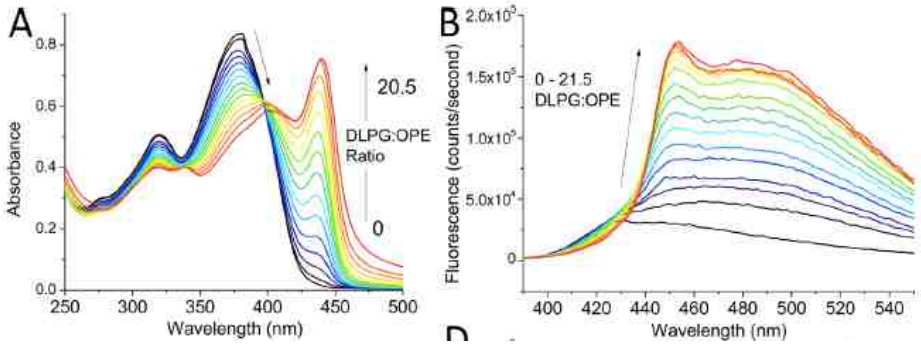

Figure 6. (left) Absorbance spectra and (right) fluorescence spectra (excitation wavelength : 375nm) of 1.4 μM +2C with DLPG. Adapted from Hill et al.

These results and others from Hill et al show that OPEs complex with oppositely-charged surfactants to form J- or H-aggregates based on differences in molecular geometry, and these complexes are highly sensitive to the solution environment.

3.3. Materials and Methods

Six phenylene-ethynylene (PE) backboned compounds were tested: S-OPE-2(COOEt), PIM-4, EO-C2 (positive) PE-SO_3-H, PE-SO_3-COOH, and PE-SO_3-COOEt (negative). Structures of these six compounds are shown in Figures 7 and 8.

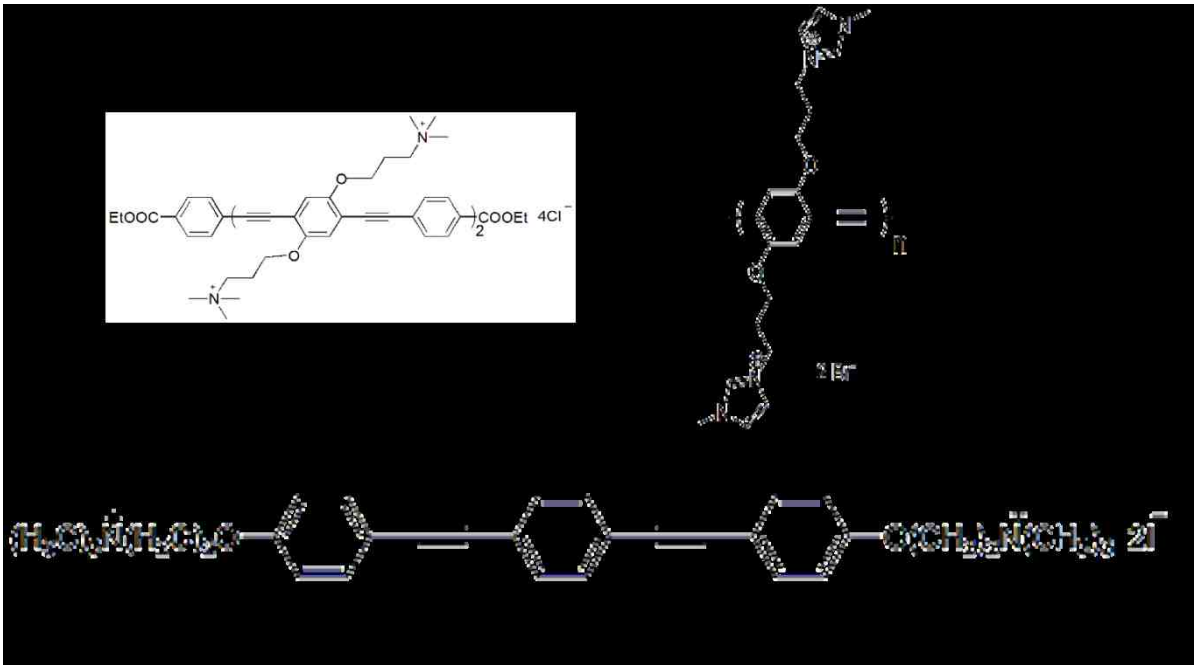

Figure 7. Positively charged PE-backboned oligomers and polymer.

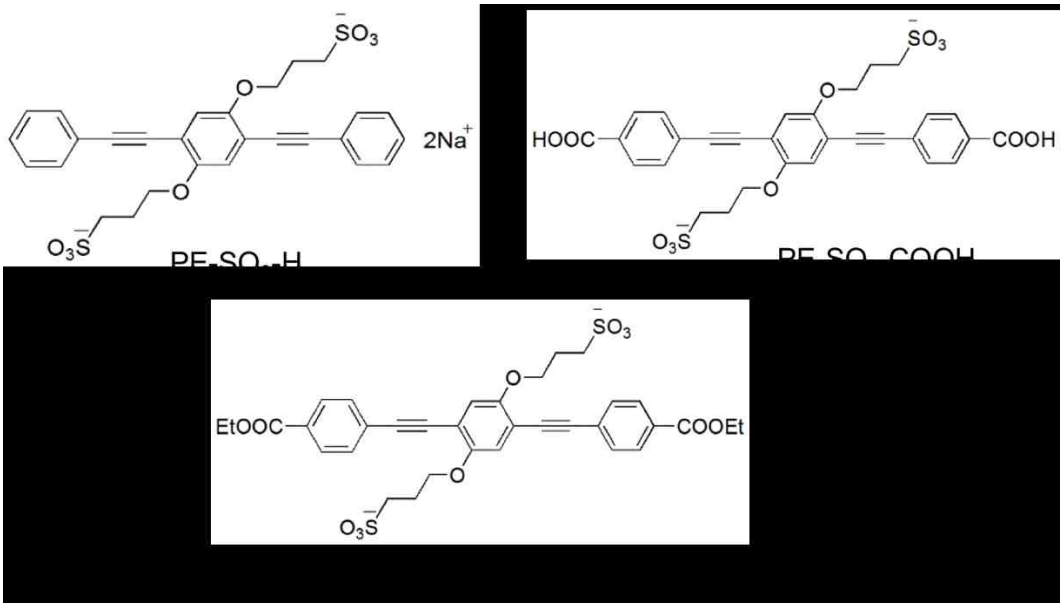

Figure 8. Negatively charged PE-backboned oligomers structures.

In order to observe the changes in fluorescence between compounds and surfactants, sodium dodecyl sulfate (SDS) with positive OPEs and tetradecyltrimethylammonium bromide(TTAB) with negative OPEs were used (surfactant structures shown in Figure 9). A concentration of 2uM in 2.5ml of DI water was used for each OPE, with varying surfactant concentrations up to 5mM. In order to observe the fluorescence changes caused by CW agents, malathion was used as a CWA mimic (structure in Figure 9). The concentrations of malathion are various, up to 0.25mM (LC_{50}). Emission spectra were measured with different excitation wavelengths based on previous work (Figure 10).[9,18,19] Then, excitation spectra were measured based on the emission maximum wavelength. Spectrophotometry was performed in fused-quartz cuvettes in a PTI QuantaMax 40 steady-state spectrophotometer, using a xenon arc lamp for illumination, grating monochromators and a single PMT detector.

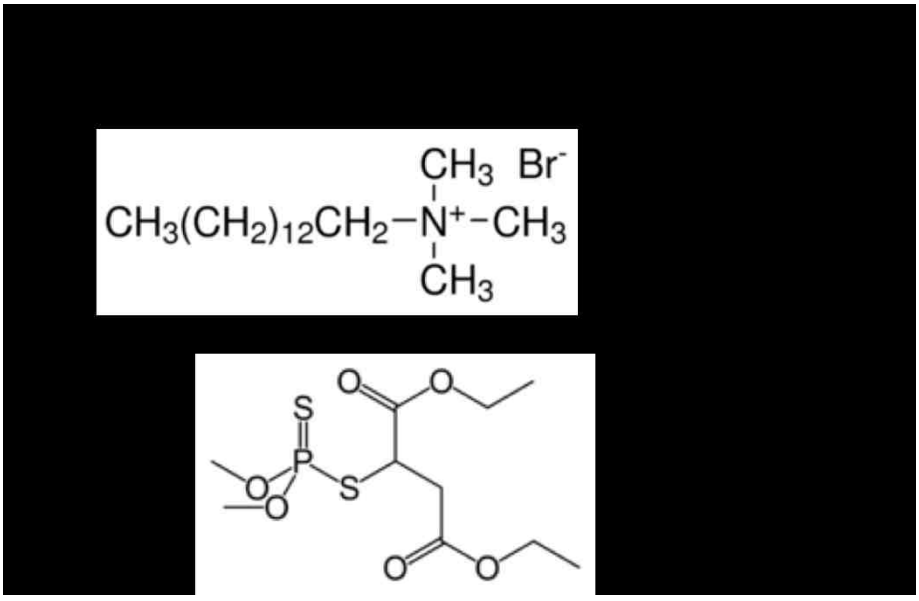

Figure 9. Molecular structures of surfactants and malathion.

Compounds	Excitation for emission spectra
S-OPE-2-COOEt	375nm
PIM-4	430nm
EO-C2	325nm
PE-SO3-H	360nm
PE-SO3-COOH	360nm

Figure 10. A Table of OPE excitation wavelengths for emission spectra.

3.4. Results

3.4.1. Positively charged OPE vs sodium dodecyl sulfate (Figure 11)

A set of spectra with S-OPE-2-COOEt (2uM) and different amounts of sodium dodecyl sulfate (SDS) shows the possibility of developing turn-on sensors. As adding more SDS, the fluorescent signals of S-OPE-2-COOEt increase because of OPE dimers formation. Turning-on point concentration ratio, S-OPE-2-COOEt to SDS, is between 0.84uM and 1.4uM, at which the ratio of OPE to SDS is 2:1. Even though the OPEs have quaternary amines as side chains, which increase the solubility of OPEs in water, S-OPE-2-COOEt molecules are acting like hydrophobic because of electron-withdrawing carboxylic ester functional groups at the end of chains.

PIM-4 vs SDS and EO-C2 vs SDS, however, show the quenching effects of surfactant. Even though fluorescence signals of PIM-4 without SDS is higher than S-OPE-2-COOEt, imidazolium groups on PIM-4 are more interactive with the surfactant molecules than quarternary amine groups on S-OPE-2-COOEt. While EO-C2 has a higher fluorescence signal

than the other two positive OPEs, the degree of quenching increased with longer light exposure, implying an end-only OPE is not the best candidate for a chemical warfare agent sensor.

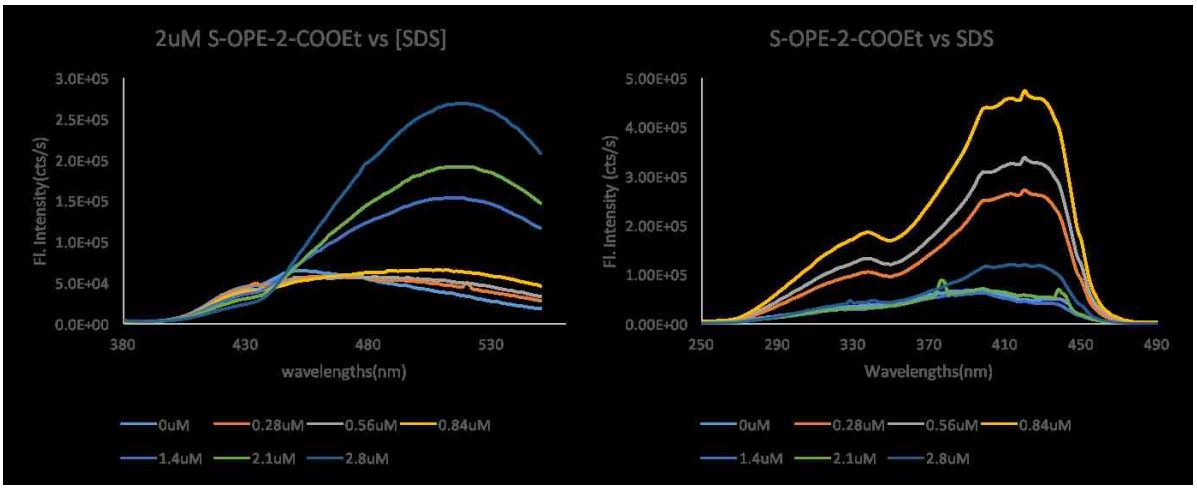

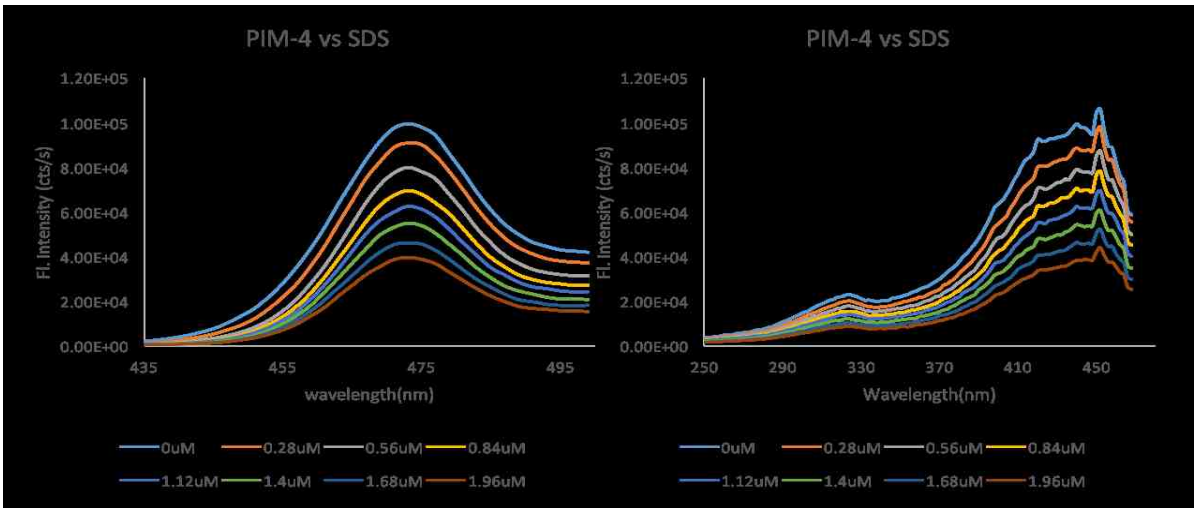

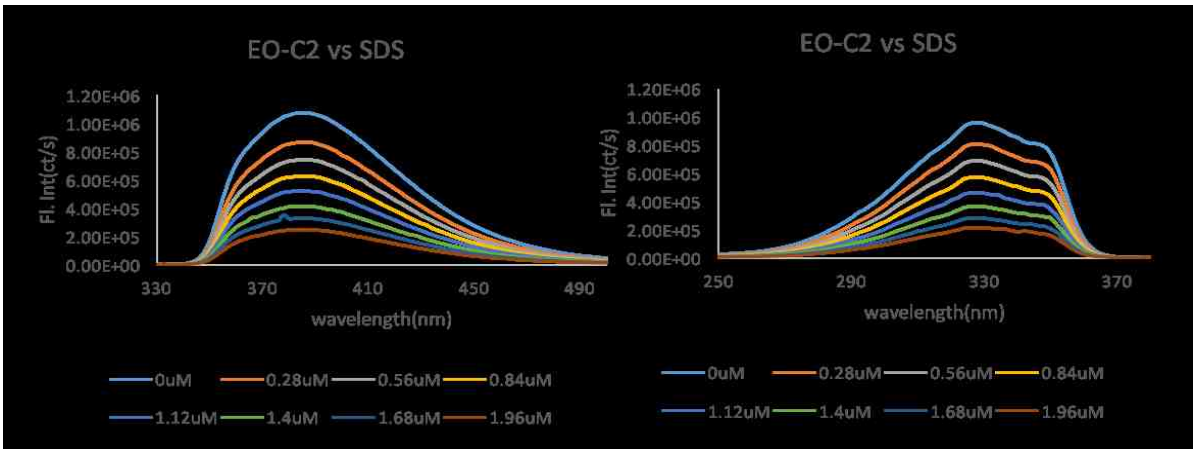

Figure 11. Positive OPEs(2uM) vs SDS emission(left) and excitation (right) spectra.

3.4.2. 2uM Positive OPE + 1.96uM SDS vs malathion (Figure 12)

All three compounds are quenched in the presence of malathion, and the quenching increases as malathion concentration increases. Spectra of S-OPE-2-COOEt (2uM) with increasing amounts of malathion show increasing fluorescence quenching effects. It can be explained that the formation of OPE dimers are interrupted by malathion. Spectra of PIM-4 on Figure 11 and 12 look similar, which implies that the interaction between PIM-4 and SDS and between PIM-4 and malathion are interrupting the electron flow along the polymer equally. The fluorescence of EO-C2 with SDS are less quenched by malathion than PIM-4 because EO-C2 has shorter OPE chains as well as quaternary amines on the end of chains. Quaternary amines on EO-C2 and S-OPE-2-COOEt are less subjective to water soluble molecules than imidazoliums.

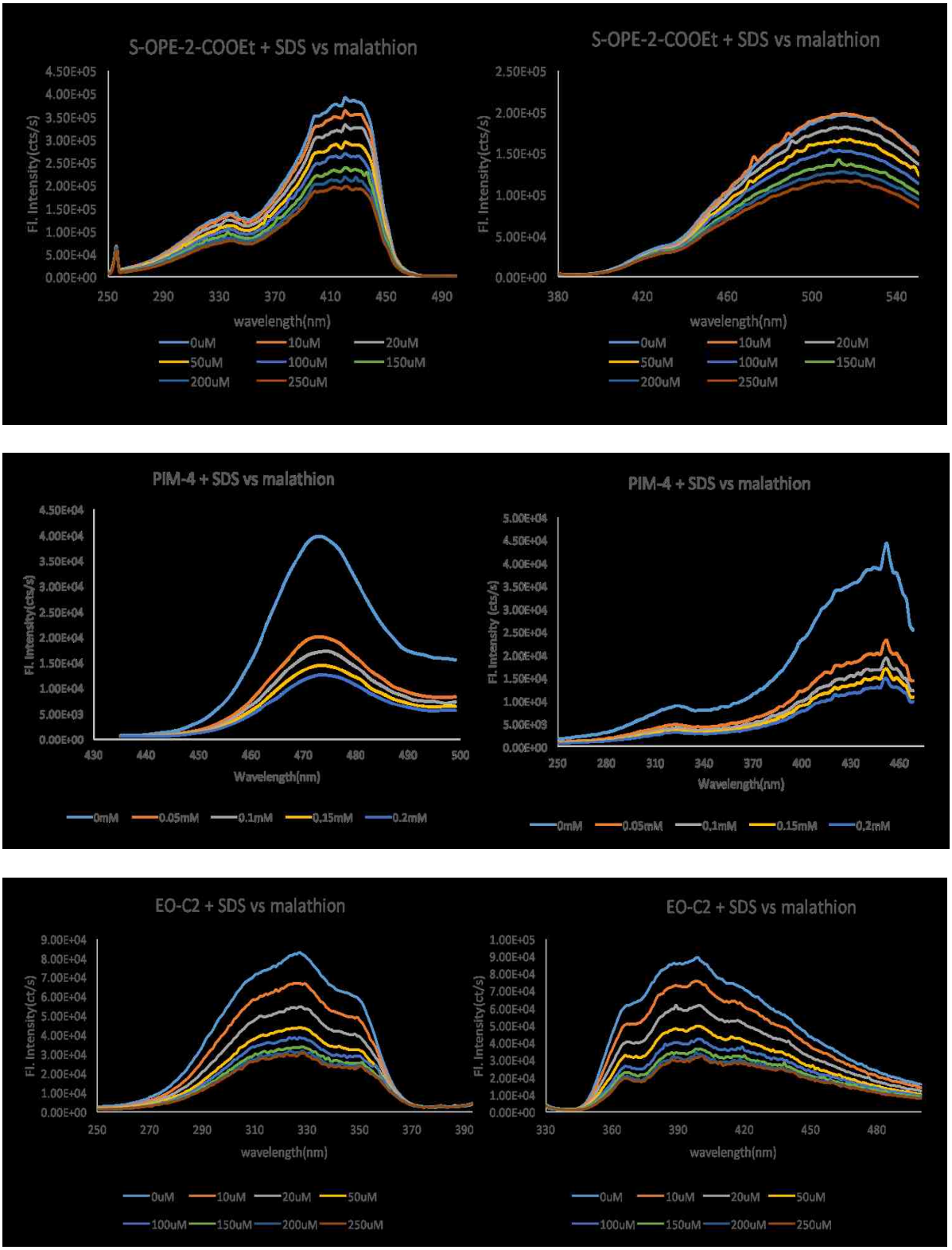

Figure 12. Positive OPEs(2uM) + SDS(1.98uM) vs malathion emission(left) and excitation (right) spectra

3.4.3. 2uM Negative OPE vs TTAB (Figure 13)

PE-SO_3-H vs TTAB and PE-SO_3-COOH vs TTAB show the quenching effects of surfactant. Even though the initial fluorescence signal of PE-SO_3-H was higher than PE-SO_3-COOH, the degree of TTAB quenching effects was similar, about five percent according to the relative fluorescence intensity ($f=F_0/F$) calculation. This is probably because the interactions between OPE and TTAB and between OPE-COOH and TTAB are similar.

A set of spectra with PE-SO_3-COOEt and different amounts of TTAB shows similar results to the cationic analogue. With increasing concentration of TTAB, the fluorescent signals of PE-SO_3-COOEt increased because of OPE dimers formation. The turning-on point concentration ratio, PE-SO_3-COOEt to TTAB, is between 0.56uM and 0.84uM, at which the ratio of OPE to TTAB is 4:1. Even though all three negative OPEs have shorter chains and functional groups on the chain ends, only PE-SO_3-COOEt with TTAB shows the fluorescence enhancement. The fluorescence yield of PE-SO_3-COOEt is highly quenched in water, and its ethyl ester end groups significantly change the hydrogen-bonding geometry and electronic structure of the dye.

3.4.4. 2uM Negative OPE + 1.96uM TTAB vs malathion (Figure 14)

Addition of malathion to OPE-TTAB complexes resulted in no significant change to the emission or excitation properties of the dye. Spectra of PE-SO_3-H and PE-SO_3-COOH on Figure 14 are similar to the ones on Figure 13, which implies that the sensitivity of the two oligomers is similar. Though fluorescence changes of PE-SO_3-COOEt are similar with the other two oligomers, which is about 6% quenching, turning-off is observed after turning-on

due to the formation of OPE dimers. The change is not large enough to form the basis for a functional sensor, however; only the cationic OPEs showed promise in this area.

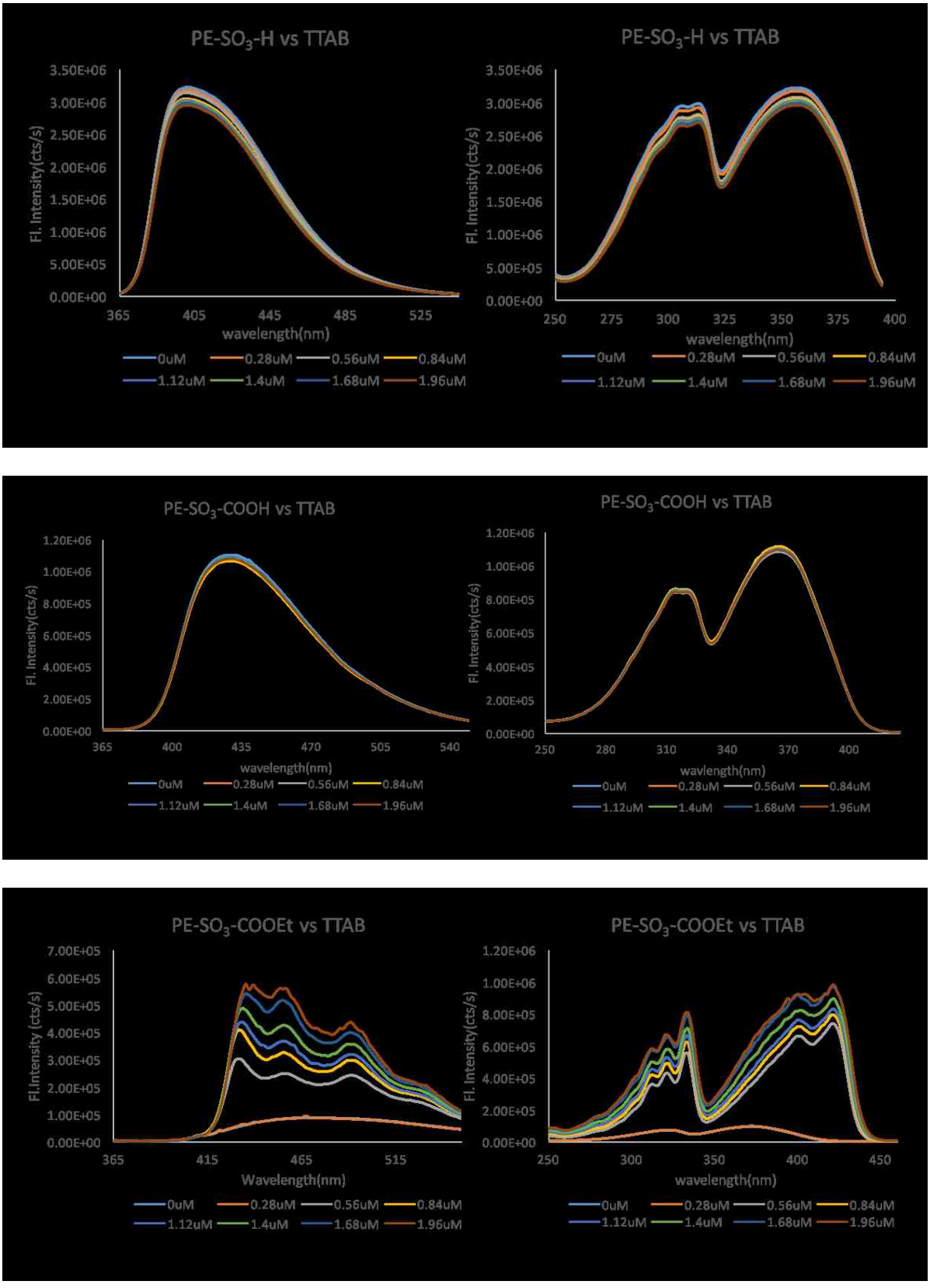

Figure 13. Negative OPEs(2uM) vs TTAB emission(left) and excitation (right) spectra.

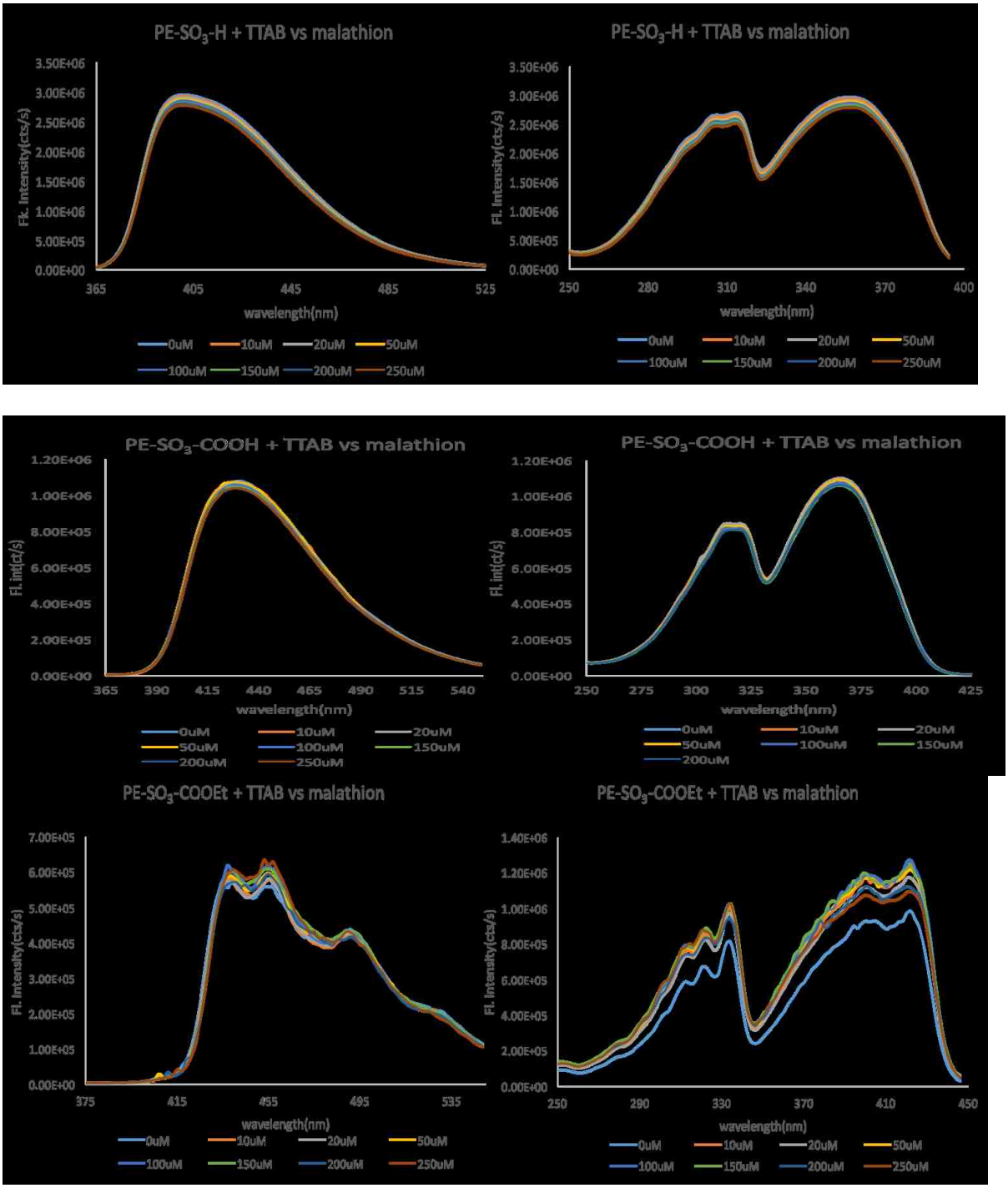

Figure 14. Negative OPEs(2uM) + TTAB(1.96uM) vs malathion emission(left) and excitation (right) spectra.

CHAPTER 4. OXIMATES AND FLUORESCENCE CHANGES

4.1. Background

Wallace et al[20] and Diaz de Grenu et al[21] reported that oximate ions can both detect chemical warfare agents and reactivate acetylcholinesterase (AChE). They modified a coumarin fluorophore with an oxime group, resulting in a molecule with very low fluorescence. But when a CW simulant, diiopropylfluorophosphate (DFP), was added, fluorescence enhancement and blue-shifted absorbance spectra were observed. The reaction between coumarin oximate and DFP is shown to be fast with a rate constant of $1410s^{-1}$ and half-life of 50ms (Figure 15). Ellin et al[22] found that CW antidotes with oximates, such as pralidoxime (2-PAM) and 1,1'-trimethylene bis(4-formylpyridinium bromide) dioxime (TMB-4), can reactivate acetylcholinesterase (AChE) by reversing the covalent modifications caused by organophosphorus agents, detaching the residues of the agents from the acetylcholinesterase (Figure 16).

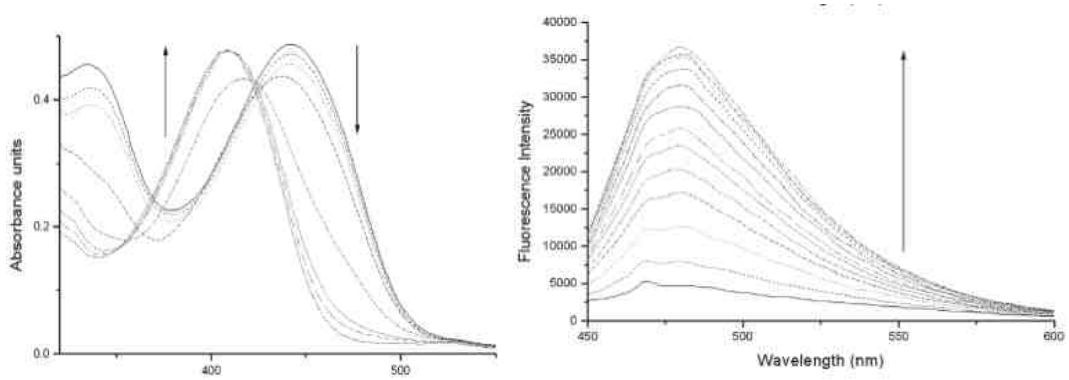

Figure 15. (Left) Absorption spectra changes of coumarin-oximate compounds as adding more DFP. (Right) Fluorescence enhancement of coumarin-oximate compounds as adding more DFP. Adapted from Wallace et al.

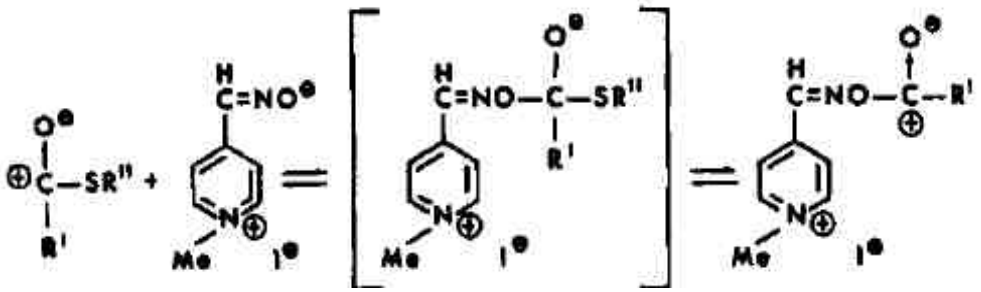

Figure 16. Reaction mechanisms of 4-PAM with chemical warfare agent. Adapted from Ellin et al.

Diaz de Grenu et al developed the chemical warfare screening model with different fluorophores and reactive functional groups (Figure 17).[21] Their results show that each chemical warfare agent and mimic molecule has unique color changes, so it is possible to identify which of many possible CWAs are present, as well as distinguish against false positive results (Figure 18). often caused by organophosphorus pesticides such as malathion. This type of chemical array allows for more robust screening and better rejection of false positives.

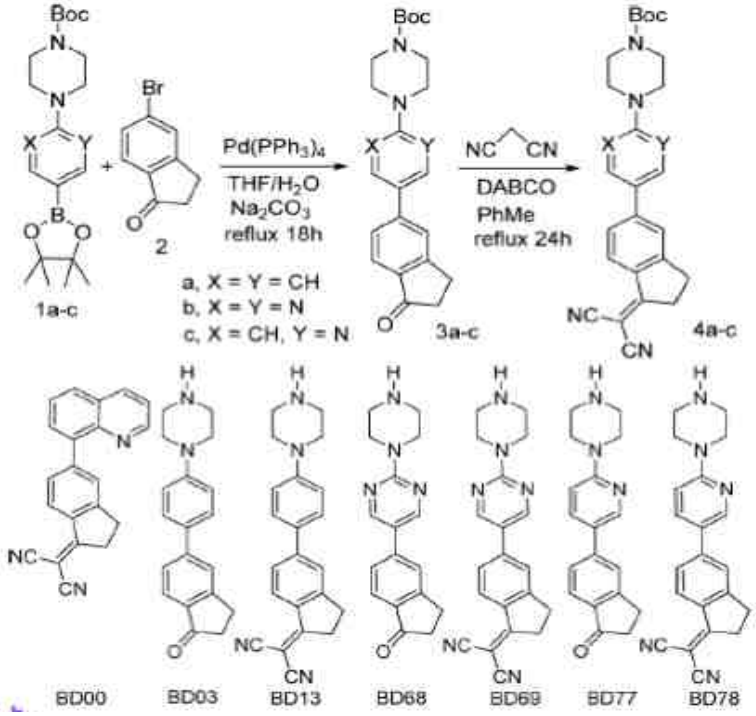

(Figure 17) A scheme of different fluorophore with various reactive functional groups. Adapted from Diaz de Grenu et al.

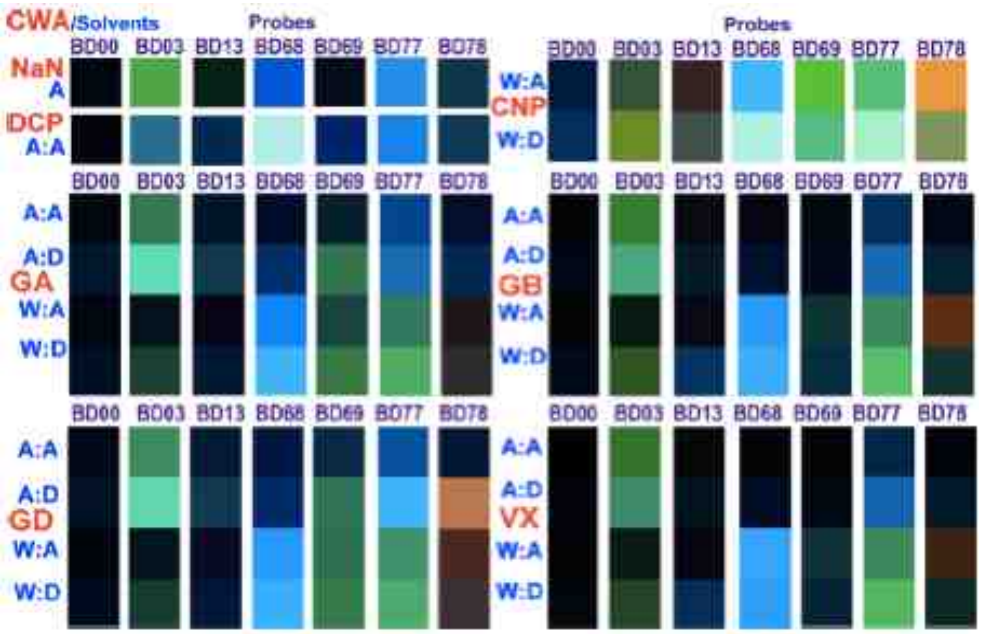

Figure 18. Observation of fluorescent color changes of different compound from figure 17. Adapted from Diaz de Grenu et al.

4.2. Oxime-OPEs as selective sensors

In addition to OPEs with COOEt functional groups, a new OPE molecule with oximates are currently being developed. Oximates are nucleophiles attacking phosphorus centers of the organophosphrous compounds. After making covalent bonds between oxygen and phosphorus, the fluorescent dyes can be turned-on due to the loss of photoinduced electron transfer from the oximate anion, as demonstrated by Wallace et al.[20]

4.2.1. Synthetic procedure

The synthesis of new oxime molecules is summarized on Figure 19. 1.16g (1 eq) of 1,4-Bis[(trimethylsilyl)ethynyl]benzene(1g, Sigma-Aldeich) was added into 150ml round flask and dissolved in 30ml DCM(CH_2Cl_2) and 30ml methanol. Then 4.73g (8 eq.) of potassium carbonate was added into the solution. The reagents were stirred at the room temperature overnight. After evaporating solvents from the flask, compounds were washed with ammonium chloride(NH_4Cl) and sodium chloride(NaCl). Then, the compound solution was dried by 4g of magnesium sulfate($MgSO_4$) overnight. The solution was filtered with DCM and the solvent were evaporated.

Synthesis of the bis-benzaldehyde OPE is ongoing. Preparation of the oxime from the aldehyde with hydroxylamine should be facile. Once the oximo-OPE is completed, testing of its pH sensitive photophysical properties will be completed, reactivity towards organophosphates determined spectroscopically and the kinetic parameters found.

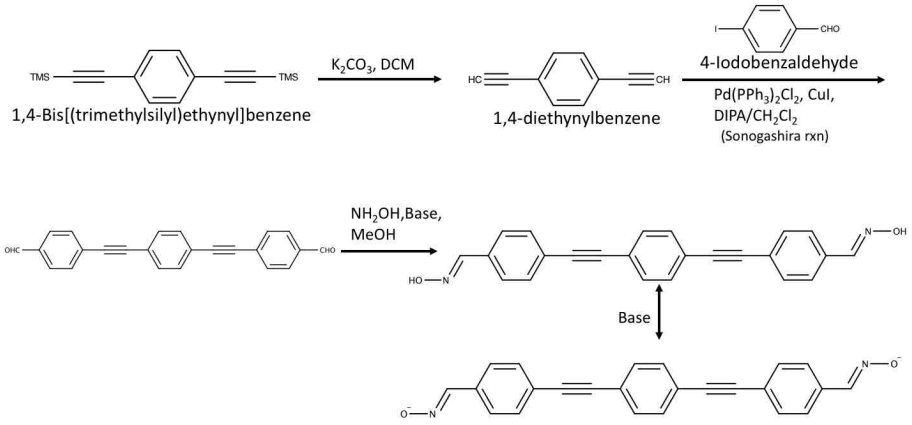

Figure 19. Synthesis steps of an end-only oximes molecule.

CHAPTER 5. DETECTING CWAs in CELLS

5.1. Background

Laser scanning microscopy is a useful biological research technique to observe cells and tissues treated by various analytes and cell stains. One-photon and two-photon laser scanning microscopy both use laser radiation to excite molecules bound to specific biological structures from the ground to the first excitation state, after which they decay by emitting a lower-energy photon (fluorescence) that is captured and transduced to an electrical signal by an appropriate detector. Two-photon microscopy has been used as an alternative for single-photon microscopy in order to improve resolution in the z direction and hence get better 3D images and to avoid light scattering in biological samples to extend the depth at which functional imaging can be done.

Even though both one-photon confocal microscopy provides high-resolution biological images, it requires the use of a pinhole to get resolution in the z-dimension, and requires excitation light that is in the range of absorption by the fluorophore. Fluorophores generally absorb and emit light in the near-UV or visible regions, to which biological samples are opaque in bulk. This fact limits the depth at which effective imaging can be performed. In order to overcome this limitation, two-photon excitation technique was developed. The difference between single-and double photon excitation is in the process used to excite the fluorophore. Whether using one or two-photon laser, the total energy used to the excite a fluorophore is the same, but two-photon excitation uses simultaneous absorption by the dye of two photons each with half the energy required to reach the exited state. This (1) allows the use of near-infrared and infrared radiation at double the usual wavelength, which is absorbed

and scattered much less by tissue, and (2) improves the vertical resolution significantly because the photon intensity is only high enough to cause excitation in a very small volume, smaller than the confocal volume created by the use of a pinhole.[23] Unlike one-photon techniques which can be performed with any laser, two-photon excitation requires the use of a very fast pulsed laser to "compress" the incident light into very small windows of time. Otherwise the continuous power output required to get sufficient light intensity to produce a two-photon excitation would destroy the sample.

The main limitation of two-photon microscopy, besides the expensive laser, is the lack of useful fluorophores with sufficient two-photon cross section. Based on their length, propensity to self-aggregate and potential for engineered charge-transfer systems, OPEs and PPEs are exciting candidates for usefully large two-photon cross section. In pursuit of intracellular detection of chemical warfare agents, a pilot study to determine if the relevant OPEs are cell-penetrant and capable of being excited with a two-photon laser was undertaken.

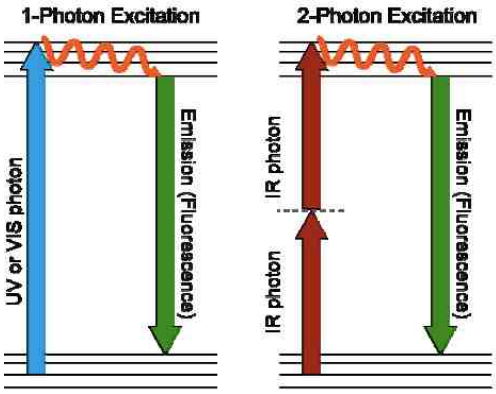

Figure 20. Diagram of one-photon and two-photon excitation. Adapted from Kurtz et al.

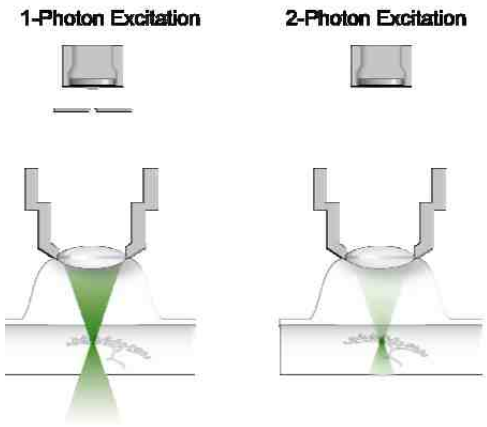

Figure 21. Illustration of focuses with one-photon and two-photon excitations. Adapted from Kurtz et al.

It has been shown that OPE molecules can be used to penetrate bacteria and mammalian cells and can be detected with single-photon confocal microscopy. Focusing on mammalian cell penetration, the experiment was designed to test whether OPEs can be used as a stain for tracking chemical warfare agent in cell organelles. It has been shown that OPEs and PPEs have high fluorescence quantum yields. Confocal microscopy with two-photon laser excitation can help to improve the resolution, especially in the z-direction, of cells and tissue images. In order to excite PPEs and OPEs and to test them for penetrating cells, two-photon laser scanning microscopy and 3t3 cells were used. Cells were penetrated by S-OPE-2-(H) molecules in less than an hour at a low concentration, between 0.1ug/ml and 10ug/ml. After cell treatment under the OPE solution, cell images were taken with the two-photon laser microscopy.

5.2. Materials and Methods

3T3 cells (NIH 3T3 Cell Line murine) were originally obtained from Sigma-Alderich (St. Louis, MO). Cells were grown in Mem-alpha-based medium to approximately 70-80% confluence (forming cell monolayer) in tissue culture polystyrene(TCPS) flasks. Medium in the cell flasks were changed every two days until the flasks reach at 80% confluence. After confluence, cells were trypsinized with 0.25% trypsin/EDTA (100ml, from ThermoFisher Scientific, Waltham, MA) and moved into new TCPS flasks with a density of 150,000 cells per a flask. Cells were incubated at 37^{o}C, 5% CO2 and ~90% relative humidity(RH). Medium was mixed with 90% MEM-alpha (500ml, from HyClone, Logan, UT), 5% Penicillin-Streptomycin (100ml, from ThermoFisher Scientific, Waltham, MA), and 5% fetal bovine serums (500ml, from Sigma-Aldrich, St. Louis, MO).

In order to take images of 3T3 cells, cells were seeded on coverslips (18mm, from VWR, Northbrook, IL) in 24-well plates at a density of 100,000 cells per well and placed in an incubator (37^{o}C, 5% CO2 and ~90% RH) overnight. Before seeding cells on coverslips, the coverslips were washed with 200 proof ethanol in covered petri dishes for 10 minutes then they were blow-dried with nitrogen gas. Before adding OPE solutions, cells were washed with PBS buffer three times. Then, cells were incubated in 2ml of S-OPE-2(H) solution, which is diluted stock solution with PBS buffer, for 30 minutes. For negative control coverslips, cells were incubated in 2ml of PBS buffer. After washing cells with 1ml PBS three times, cells were grown in 2ml of diluted Syto 21 green (5mM, 250ul, from Life Technologies, Carlsbad, CA) with PBS buffer. Cells were fixed with 2% glutaraldehyde 200ul after being washed with 1ml PBS buffer three times. Coverslips were placed inverted on the glass slides (25X75mm,

1.0mm thick, VWR, Northbrook, IL) with 15ul Prolong Diamond antifade mountant (2ml, from Life Technologies, Carlsbad, CA).

In order to take cell images, LSM 510 two-photon microscope were used with an objective of 40X oil immersion. Samples with OPE molecules were excited by 725nm (IR laser) with 364mW (13% of maximal power). To excite Syto 21 stain, the excitation wavelength was chosen at 488nm(Ar) with 13.5mW (45% of maximal power). DAPI (BP 435-485nm) and FITC (LP 505) filters were used for OPEs and Syto 21 respectively.

5.3. Results

In order to find the position of nucleic acid in the 3T3 cells, Syto 21 stain was used as a marker. As shown figure 22, nucleic acids are located in the middle of cell core and the stain is not shown under DAPI filter. After 30minutes exposure with the concentration of 10ug/ml, S-OPE-2(H) compounds are visible throughout the cell (Figure 23). In order to define the preferred binding sites for S-OPE-2(H) in the cells, the concentration of the OPE was varied during cell preparation. With 1ug/ml and 0.1ug/ml OPE concentration, the OPE compounds are clustered in the middle of cell core, showing that the OPEs bind preferentially to nucleic acid (Figure 24). This result shows that even low concentration of OPEs can penetrate cells within 30 minutes as well as that the compound can be excited by two-photon processes.

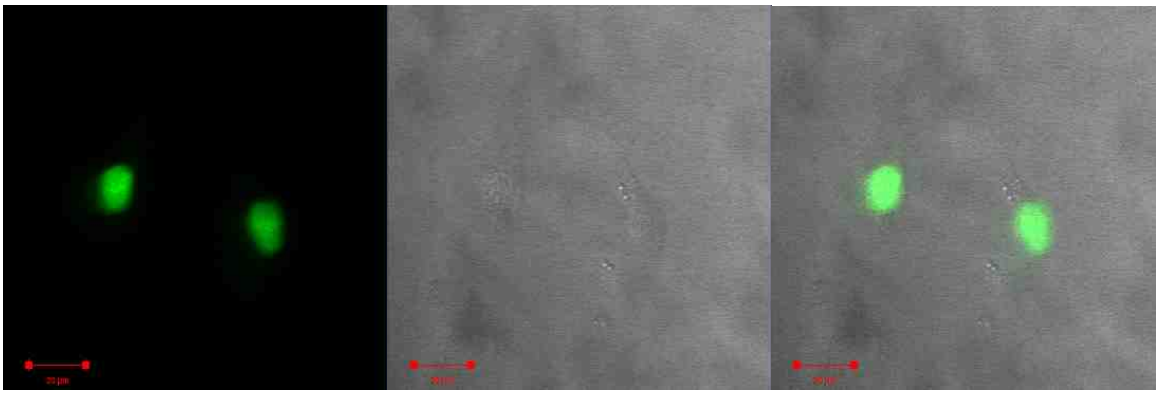

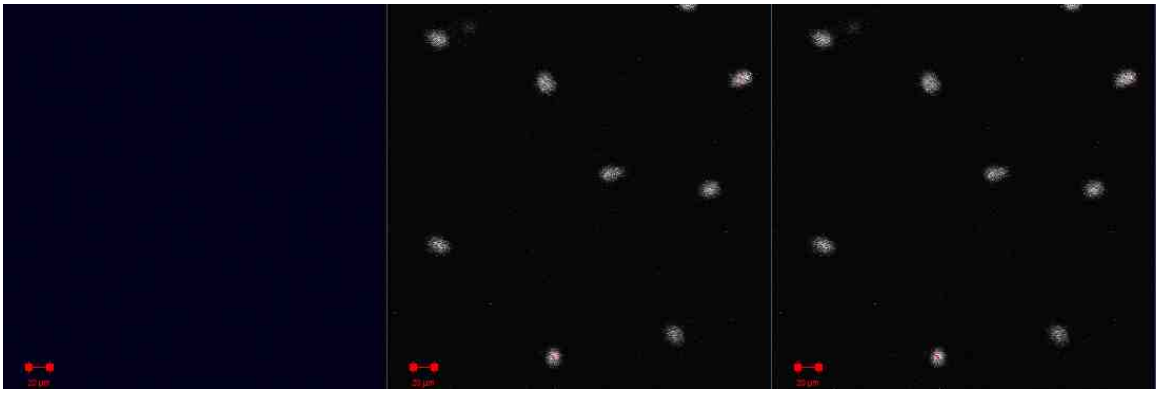

Figure 22. Non-OPE treated 3T3 cells with syto 21 stain. (Top left to right) Syto 21 channel, DIC images, and merged. (Bottom left and right) Under DAPI and FITC filter. All scale bars on images are 20um.

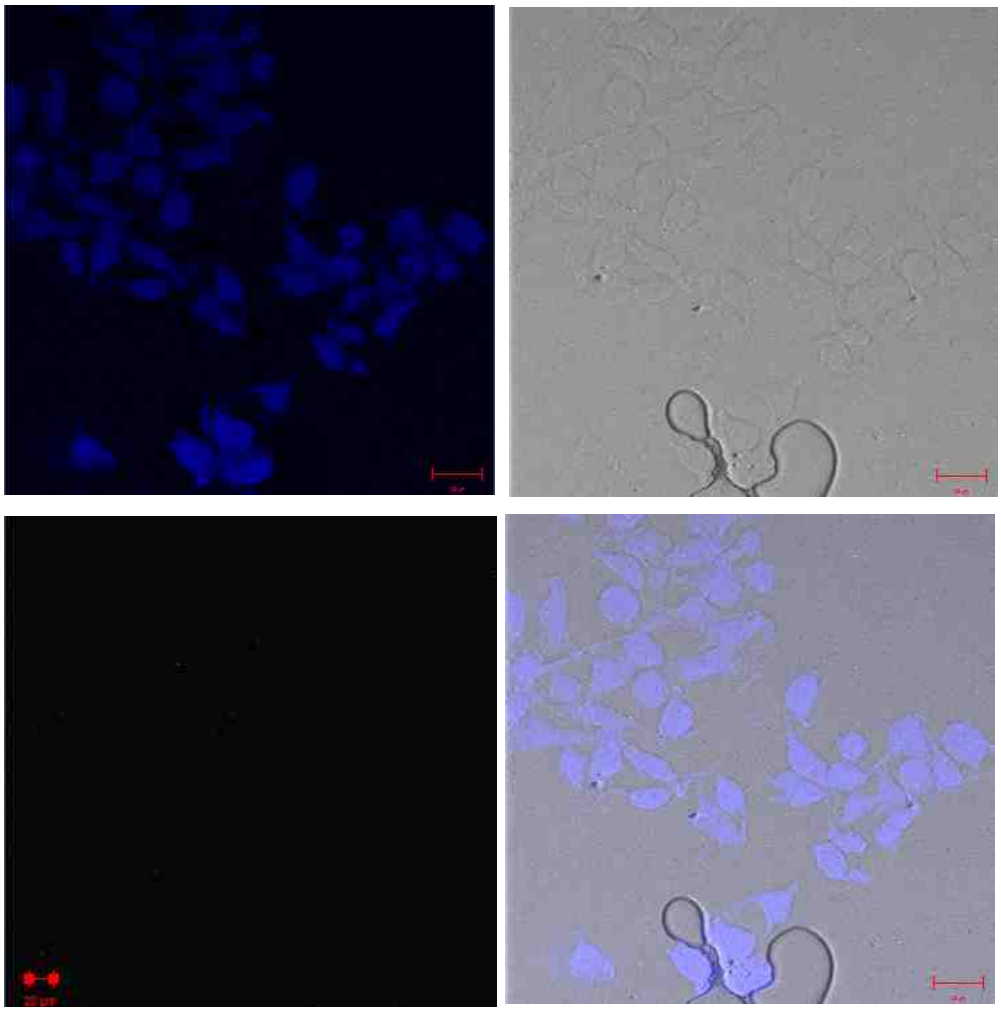

Figure 23. Images of 3T3 cells with 10ug/ml OPE treatment for 30 minutes. (Clockwise from the top left) images under DAPI, DIC, merged and FITC filters. All scales on the images are 20um.

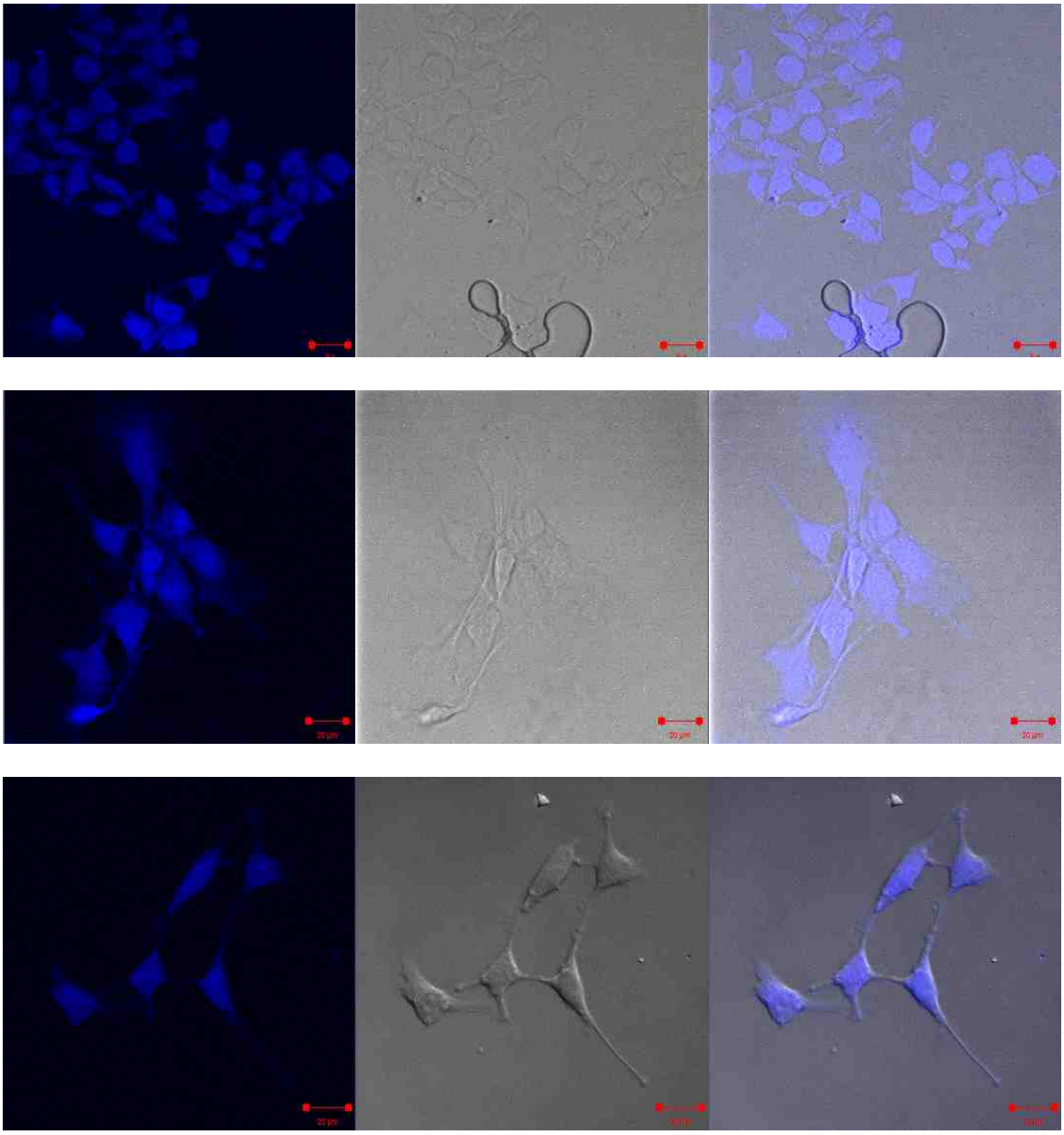

Figure 24. Images of 3T3 cells treated with (a)10ug/ml, (b)1ug/ml, and (c) 0.1ug/ml S-OPE-2(H). Each image set has the arrangement of DAPI filter, DIC, and merged (from left to right). All image scales are 20um.

Imaging of OPE-treated NIH 3T3 cells under two-photon excitation shows clearly that OPEs will penetrate cells and do not bind strongly to any particular structure. The two-photon excitation was capable of exciting OPE fluorescence which is a valuable proof of concept for further studies. Despite their cell penetration, OPEs have been shown not to exert any significant toxic effects on mammalian cells, indicating that their presence in the cell is relatively benign. These results, and the techniques used to obtain them, should prove useful in further development of OPE-based intracellular assays for a variety of analytes.

CHAPTER 6. Conclusions

For years, we have developed the applications of oligo phenylene-ethynylenes against biological warfare agent, bacteria. We successfully demonstrated that the biocidal activities of OPEs are moderately effective under different temperatures ($4^{O}C$ or $25^{O}C$) and different compositions (PPE + PNIPAAm, PPE only, negative control). New applications of OPE/surfactant systems as sensors for CW agents has been demonstrated, based on disruption of surfactant-mediated OPE dimers by CWA mimics. A proposed new sensor based on covalent reaction between oximate ions and organophosphorus CW agents is also under development.

Among six high fluorescent dye molecules, the most effective dyes sensing malathion are S-OPE-2-COOEt and PE-SO_3-COOEt because of turn-on and off mechanisms depending on the solution conditions. When adding more surfactants to the OPE solutions, the fluorescence of both molecules increased over six-fold vs. negative control (no surfactants) because of J-dimer formation and dequenching. The turning-on concentration ratios, OPE to surfactant, are 2:1 for positive OPEs and 4:1 for negative OPEs. As more malathion is added to the OPE aggregation solutions, the fluorescence is decreased, possibly because the malathion interrupt OPEs from aggregating with each other.

Even though S-OPE-2(H) is shown to penetrate mammalian cells and to undergo efficient two-photon excitation, other positively charged OPEs should be tested in order to develop cell organelle track stains. In order to track the pathways of chemical agents in vivo, imaging with live cells is needed to be performed. For understanding mechanisms of J-aggregate formation and disaggregation in the presence of surfactants and malathion further, more experimental data such as computational calculation is needed to be supported. Currently,

a new OPE molecule with oximate functional groups is being synthesized and the measurements of absorbance and fluorescence changes and lifetime in the presence of organophosphorus compounds will be performed. Hopefully this project will lead to a useful advance in the detection of CWAs with one- and two-photon excitation. The results of this work shows the flexibility and power of self-assembling fluorescent amphiphiles in perturbing and reporting on biological systems.

REFERENCES

1. Burnworth, M., Rowan, S.J., and Weder, C. Fluorescent Sensors for the Detection of Chemical Warfare Agents. *Chem. Eur. J.* 2007, 13, 7828 – 7836.

2. Sonogashira, K., Tohda, Y., and Hagihara, N. A Convenient Synthesis of Acetylenes : Catalytic Substitutions of Acetylenic Hydrogen with Bromoalkenes, Iodoarenes, and Bromopyridines. *Tetrahedron Lett.* 1975, 50, 4467 – 4470.

3. Wohrle, D., and Meissne, D. Organic Solar Cells. *Adv. Mater.* 1991, 3, 129 – 138.

4. Wang, Y., Chi, E. Y., Schanze, K.S., and Whitten, D.G. Membrane activity of antimicrobial phenylene ethynylene based polymers and oligomers. *Soft Matter.* 2012, 8, 8547 - 8558.

5. Pappas, H.C., Donabedian, P. L., Schanze, K.S., and Whitten, D.G. Intended and Unintended Consequences and Applications of Unnatural Interfaces: Oligo p-Phenylene Ethynylene Electrolytes, Biological Cells and Biomacromolecules. *J. Braz. Chem. Soc.* 2015, 00(00), 1 - 11.

6. Wang, Y., Jett, S. D., Crum, J., Schanze, K.S., Chi, E. Y., Whitten, D. G. Understanding the Dark and Light-Enhanced Bactericidal Action of Cationic Conjugated Polyelectrolytes and Oligomers. *Langmuir*, 2013, 29(2), 781 – 792.

7. Chen, L., McBranch, D. W., Wang, H., Helgeson, R., Wudl, F., and Whitten, D. G. Highly sensitive biological and chemical sensors based on reversible fluorescence quenching in a conjugated polymer. *Proc Natl Acad Sci*. 1999, 96(22), 12287–12292.

8. Tang, Y., Achyuthan, K.E., and Whitten, D.G. Label-free and Real-Time Sequence Specific DNA Detection Based on Supramolecular Self-assembly. *Langmuir*, 2010, 26(9), 6832 – 6837.

9. Hill, E. H., Sanchez, E., Evans, D.G, Whitten, D.G. Structural Basis for Aggregation Mode of oligo-p-Phenylene Ethynylenes with Ionic Surfactants. *Langmuir.* 2013, 29, 15732−15737.

10. Hill, E. H., Zhang, Y., Evans, D. G., and Whitten, D.G. Enzyme-Specific Sensors via Aggregation of Charged p-Phenylene Ethynylenes. *ACS Appl. Mater. Interfaces*. 2015, 7, 5550 − 5560.

11. Donabedian, P. L., Pham, T. K, Whitten, D.G., and Chi, E. Y. Oligo (p-phenylene ethynylene) Electrolytes: A Novel Molecular Scaffold for Optical Tracking of Amyloids. *ACS Chem. Neurosci.* 2015, 6 (9), 1526 – 1535.

12. Parthasarathy, A., Ahn, H., Belfield, K. D., and Schanze, K. S. Two-Photon Excited Fluorescence of a Conjugated Polyelectrolyte and Its Application in Cell Imaging. *ACS Appl. Mater. Interfaces.* 2010, 2 (10), 2744 – 2748.

13. Pappas, H. C., Phan, S., Yoon, S., Edens, L. E., Meng, L., Schanze, K. S., Whitten, D. G., and Keller, D. J. Self-Sterilizing, Self-Cleaning Mixed Polymeric Multifunctional Antimicrobial Surfaces. *ACS Appl. Mater. Interfaces* 2015, 7, 27632 − 27638.

14. Akiyama, Y. Kikuchi, A., Yamato, M., and Okano, T. Ultrathin Poly(N-isopropylacrylamide) Grafted Layer on Polystyrene Surfaces for Cell Adhesion/Detachment Control. *Langmuir* 2004, 20, 5506 - 5511.

15. Zwiener, R. J., and Ginsburg, C. M. Organophosphate and Carbamate Poisoning in Infants and Children. *Pediatr.* 1988. 81(1), 121 - 126.

16. Askew, B. M. Oximes and Atropine in Sarin Poisoning. *Brit. J. Pharmacol.* 1957, 12, 340 - 343.

17. Eisfeld, A., and Briggs, J. S. The J- and H-bands of organic dye aggregates. *J. Chen. Phys.* 2006, 324(2), 376 – 384.

18. Hill, E. H., Evans, D. G., and Whitten, D. G. Photochemistry of "End-Only" Oligo-*p*-phenylene Ethynylenes: Complexation with Sodium Dodecyl Sulfate Reduces Solvent

Accessibility. *Langmuir*, 2013, 29(31), 9712 – 9720.

19. Parthasarathy, A., Pappas, H. C., Hill, E. H., Huang, Y., Whitten, D. G., and Schanze, K. S. Conjugated Polyelectrolytes with Imidazolium Solubilizing Groups Properties and Application to Photodynamic Inactivation of Bacteria. *ACS Appl. Mater. Interfaces*, 2015, 7 (51), 28027 – 28034.

20. Wallace, K. J., Fagbemi, R. I., Folmer-Andersen, F. J., Morey, J., Lynth, V. M., and Anslyn, E. V. Detection of chemical warfare simulants by phosphorylation of a coumarin oximate. *Chem. Commun.,* 2006, 3886 -3888.

21. Diaz de Grenu, B., Moreno, D., Torroba, T., Berg, A., Gunnars, J., Nilson, T., Nyman, R., Persson, M., Pettersson, J., Eklind, I., and Wasterbv, P. Fluorescent Discrimination between Traces of Chemical Warfare Agents and Their Mimics. *J. Am. Chem. Soc.* 2014, 136 (11), 4125 – 4128.

22. Ellin, R. I., and Wills, J. H. Oximes Antagonistic to Inhibitors of Cholinesterase. *J. Pharm. Sci.* 1964, 53(10), 1143 - 1150.

23. Kurtz, R. Bright Solutions to Get Sharp Images: Confocal and Two-Photon Fluorescence Microscopy and the Pros and Cons of New Multifocal Approaches. *Modern Research and Educational Topics in Microscopy*. 2007, 154 - 163.